



Article

Antioxidant Activity of Ruthenium Cyclopentadienyl Complexes Bearing Succinimidato and Phthalimidato Ligands

 Michał Juszcak ¹, Magdalena Kluska ¹, Aneta Kosińska ², Bogna Rudolf ² and Katarzyna Woźniak ^{1,*}

¹ Department of Molecular Genetics, Faculty of Biology and Environmental Protection, University of Lodz, 90-236 Lodz, Poland; michal.juszcak@edu.uni.lodz.pl (M.J.); magdalena.kluska@edu.uni.lodz.pl (M.K.)

² Department of Organic Chemistry, Faculty of Chemistry, University of Lodz, 91-403 Lodz, Poland; aneta.kosinska@chemia.uni.lodz.pl (A.K.); bogna.rudolf@chemia.uni.lodz.pl (B.R.)

* Correspondence: katarzyna.wozniak@biol.uni.lodz.pl

Abstract: In these studies, we investigated the antioxidant activity of three ruthenium cyclopentadienyl complexes bearing different imidato ligands: (η^5 -cyclopentadienyl)Ru(CO)₂-*N*-methoxysuccinimidato (**1**), (η^5 -cyclopentadienyl)Ru(CO)₂-*N*-ethoxysuccinimidato (**2**), and (η^5 -cyclopentadienyl)Ru(CO)₂-*N*-phthalimidato (**3**). We studied the effects of ruthenium complexes **1–3** at a low concentration of 50 μ M on the viability and the cell cycle of peripheral blood mononuclear cells (PBMCs) and HL-60 leukemic cells exposed to oxidative stress induced by hydrogen peroxide (H₂O₂). Moreover, we examined the influence of these complexes on DNA oxidative damage, the level of reactive oxygen species (ROS), and superoxide dismutase (SOD) activity. We have observed that ruthenium complexes **1–3** increase the viability of both normal and cancer cells decreased by H₂O₂ and also alter the HL-60 cell cycle arrested by H₂O₂ in the sub-G1 phase. In addition, we have shown that ruthenium complexes reduce the levels of ROS and oxidative DNA damage in both cell types. They also restore SOD activity reduced by H₂O₂. Our results indicate that ruthenium complexes **1–3** bearing succinimidato and phthalimidato ligands have antioxidant activity without cytotoxic effect at low concentrations. For this reason, the ruthenium complexes studied by us should be considered interesting molecules with clinical potential that require further detailed research.

Keywords: succinimide; phthalimide; ruthenium metallocarbonyl complexes; DNA oxidative damage; ROS; SOD activity; cell cycle; hydrogen peroxide



Citation: Juszcak, M.; Kluska, M.; Kosińska, A.; Rudolf, B.; Woźniak, K. Antioxidant Activity of Ruthenium Cyclopentadienyl Complexes Bearing Succinimidato and Phthalimidato Ligands. *Molecules* **2022**, *27*, 2803. <https://doi.org/10.3390/molecules27092803>

Academic Editor: Artur M. S. Silva

Received: 18 March 2022

Accepted: 24 April 2022

Published: 28 April 2022

Publisher's Note: MDPI stays neutral with regard to jurisdictional claims in published maps and institutional affiliations.



Copyright: © 2022 by the authors. Licensee MDPI, Basel, Switzerland. This article is an open access article distributed under the terms and conditions of the Creative Commons Attribution (CC BY) license (<https://creativecommons.org/licenses/by/4.0/>).

1. Introduction

In recent years, many different ruthenium complexes exhibiting various chemical and biological properties have been synthesized [1]. Complexes with anticancer potential are of particular interest [2–4]. Ruthenium complexes exhibit many features that are desirable among cancer drug candidates. They are less cytotoxic to normal cells compared to cancer cells, in which they can accumulate due to uptake by transferrin receptors. Many of them are active against cells that are metastatic and resistant to conventional chemotherapy. We recently demonstrated that ruthenium complex (η^5 -cyclopentadienyl)Ru(CO)₂(η^1 -*N*-maleimidato) has anticancer potential [4,5]. This complex was about ten times more cytotoxic to leukemic HL-60 cells compared to normal peripheral blood mononuclear cells (PBMCs). Moreover, complex (η^5 -cyclopentadienyl)Ru(CO)₂(η^1 -*N*-maleimidato) induced DNA damage and apoptosis in HL-60 cells.

Many ruthenium complexes show antioxidant activity [6–12]. For example, there are two new ruthenium complexes *cis*-[Ru(NO₂)(bpy)₂(5NIM)]PF₆ and *cis*-[RuCl(bpy)₂(MTZ)]PF₆, where bpy = 2,2'-bipyridine, 5NIM = 5-nitroimidazole, and MTZ = metronidazole have antioxidant properties in vitro. It was shown that these complexes reduced lipid peroxidation and decreased intracellular ROS levels with comparable effectiveness to the standard steroidal drug dexamethasone or α -tocopherol [9]. Similarly, radical scavenging studies

revealed that ruthenium heterocyclic complexes have high activities toward the neutralization of NO and DPPH• (2,2-diphenyl-1-picrylhydrazyl) radicals [11]. Organoruthenium(II) complexes, synthesized and analyzed by Mohankumar et al. [8], effectively scavenged the DPPH• radicals compared to that of standard control ascorbic acid. Moreover, it was shown that some of these complexes also exhibited an excellent *in vivo* antioxidant activity as they were able to increase the survival of worms exposed to lethal oxidative and thermal stresses by reducing the intracellular ROS levels. The gene expression analysis revealed that these ruthenium complexes maintained the intracellular redox status and offered stress protection through the transactivation of antioxidant defense machinery genes *gst-4* and *sod-3*, which are directly regulated by SKN-1 and DAF-16 transcription factors, respectively [8].

Studies have also shown that some ruthenium complexes have a protective effect on the cardiovascular system [13]. For example, it was revealed that a ruthenium *p*-cymene complex with quercetin binds to 3-hydroxy-3-methyl-glutaryl-CoA reductase (HMGR) both *in silico* and *in vitro* and reduces the activity of this endoplasmic, reticulum-bound enzyme that regulates the early stages of cholesterol biosynthesis [14]. It was also observed that this complex had an activity significantly higher than pure quercetin and comparable to those observed for two model drugs, pravastatin and simvastatin. Other ruthenoflavonoid complexes—[Ru(*p*-cym)(chrysin)Cl] and [Ru(*p*-cym)(thiochrysin)Cl]—showed good anti-aggregating activity in washed platelet samples [15]. The complexes were further demonstrated to interfere with several inter-platelet signaling pathways involved in aggregation, such as the integrin α IIb β 3 inside-out and outside-in signaling paths, the phosphoinositide 3-kinase (PI3K) pathway, and the release of granules. Moreover, Ru[Ru(*p*-cym)(thiochrysin)Cl] has been able to inhibit *in vitro* thrombus formation and it was shown to affect haemostasis in mice [15]. It was also found that a mononuclear ruthenium(II) diimine complex along with dietary intervention possesses cardioprotective effects in high-fat high carbohydrate diet-induced prediabetic rats by ameliorating oxidative stress and antioxidant defense enzymes, reducing MAP, restoring the heart to body weight ratio, attenuating derangement in the lipid profile and reducing cardiac inflammatory markers [16].

Recently, we demonstrated that ruthenium complexes (η^5 -cyclopentadienyl)Ru(CO)₂-*N*-methoxysuccinimidato (1), (η^5 -cyclopentadienyl)Ru(CO)₂-*N*-ethoxysuccinimidato (2), and (η^5 -cyclopentadienyl)Ru(CO)₂-*N*-phthalimidato (3) (Figure 1) showed no cytotoxic and genotoxic properties as opposed to the maleimide ligand complex [5]. Moreover, an increase in cell viability was observed after incubation with these complexes. Our comparative studies with free maleimides and succinimides and their derivatives showed that the different biological activity of ruthenium complexes depends mainly on maleimide and succinimide ligands bound to the ruthenium atom [5].

Our previous results prompted us to investigate the antioxidative activity of ruthenium complexes bearing succinimidato and phthalimidato ligands 1–3 (Figure 1) in normal and leukemia cells. Many succinimide derivatives synthesized in recent years show anti-free radical properties and are being investigated for their potential use against neurodegenerative disorders such as Alzheimer's disease, cancer, diabetes mellitus, and worms [17–20]. Here, we incubated human peripheral blood mononuclear cells (PBMCs) and HL-60 leukemic cells with hydrogen peroxide (H₂O₂) to induce oxidative stress. Incubation with H₂O₂ was preceded by pre-incubation of cells with ruthenium complexes 1–3. For comparison, we also pre-incubated the cells with ruthenium chloride (RuCl₃) and succinimide ligand. We investigated the influence of ruthenium complexes 1–3 on viability, cell cycle, and DNA oxidative damage. We also determined their effect on the level of reactive oxygen species (ROS) and superoxide dismutase (SOD) activity.

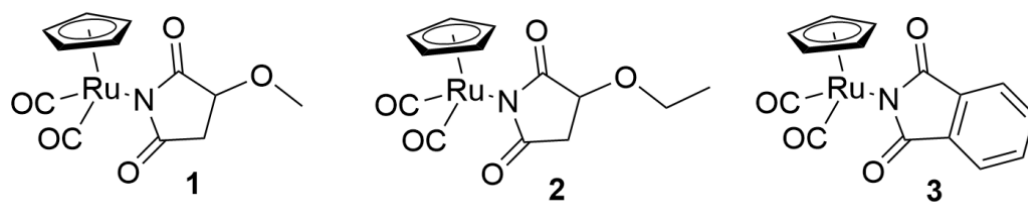


Figure 1. The structures of the ruthenium complexes 1–3.

2. Material and Methods

2.1. Chemicals

Ruthenium complexes 1–3 were synthesized as previously described (1) [21], (2) [22], (3) [5]. IMDM medium and fetal bovine serum (FBS) were obtained from Biowest (Cytogen, Zgierz, Poland). Ruthenium chloride (RuCl_3), 2',7'-dichlorofluorescein (H_2DCFDA), Hank's balanced salt solution (HBSS), dimethyl sulfoxide (DMSO), and hydrogen peroxide (H_2O_2) were purchased from Sigma-Aldrich (St. Louis, MO, USA). Succinimide was purchased from Fluka. All other chemicals were of the highest commercial grade available. A stock solution of complexes and succinimide (10 mM) was dissolved in DMSO.

2.2. Cell Culture

HL-60 (human promyelocytic leukemia) cell line was obtained from the American Type Culture Collection (ATCC) and cultured in Iscove's Modified Dulbecco's Medium (IMDM) with 15% fetal bovine serum, streptomycin/penicillin solution (100 $\mu\text{g}/\text{mL}$ and 100 U/mL). HL-60 cells were cultured in flasks at 37 °C in 5% CO_2 and sub-cultured every 2–3 days to maintain exponential growth.

Peripheral blood mononuclear cells (PBMCs) were isolated from the buffy coats obtained from healthy donors from Central Blood Bank, Lodz. Each donor agreed to donate blood. The first step of isolation of PBMCs was a mix of fresh blood from buffy coats with PBS at ratio 1:1. In the next step, the mixture was centrifuged in a density gradient of Lymphosep (Cytogen, Zgierz, Poland) at 2200 RPM for 20 min with the lowest values of acceleration and deceleration. Then the cells were washed three times by centrifugation with 1% PBS. After isolation cells were suspended in RPMI 1640 medium. The study protocol was approved by the Committee for Research on Human Subjects of the University of Lodz (17/KBBN-UŁ/III/2019).

2.3. Cell Viability

The cell viability resazurin assay was performed similarly to the method described by O'Brien et al. [23]. Resazurin salt powder was dissolved in sterile PBS buffer. PBMCs and HL-60 cells were seeded on 6-well plates at a density of 0.5×10^6 cells/mL. Cells were pre-incubated with ruthenium complexes 1–3, succinimide, and RuCl_3 at a concentration of 50 μM for 24 h at 37 °C in 5% CO_2 . Next, cells were washed with warm PBS. Then, cells were seeded on a 96-well plate in the count of 50,000 for PBMCs and 15,000 for HL-60 cells. Next, cells were incubated with H_2O_2 at concentrations of 0.2, 0.4, and 0.6 mM for 4 h at 37 °C in 5% CO_2 . Next, 10 μL of resazurin salt was added to each well, and the plates again were incubated at 37 °C in 5% CO_2 for 2 h. After that, fluorescence was measured with HT microplate reader Synergy HT (Bio-Tek Instruments, Winooski, VT, USA) using $\lambda_{\text{ex}} = 530/25$ nm and an $\lambda_{\text{em}} = 590/35$ nm. The effects of ruthenium complexes, RuCl_3 , and succinimide on cell viability were quantified as the percentage of control fluorescence.

2.4. Cell Cycle

HL-60 cells were seeded on 6-well plates at a density of 0.5×10^6 cells/mL. The cells incubated with 100 ng/mL nocodazol (NOC) for 24 h at 37 °C were the positive control. The cells were incubated with ruthenium complexes 1–3, succinimide, and RuCl_3 at a concentration of 50 μM for 24 h at 37 °C in 5% CO_2 . Next, cells were washed with warm

PBS. Then, cells were again seeded on 6-well plates. Next, cells were incubated with H₂O₂ at concentrations of 0.1 and 0.2 mM for 24 h at 37 °C in 5% CO₂. Then, cells were collected and washed twice with PBS. After that, cells were resuspended in PBS and put on ice for 15 min. Then, one volume of −20 °C absolute ethanol was added and the samples were stored at 4 °C. Before the analysis, samples were resuspended in 300 µL of staining solution containing 40 µg/mL PI (propidium iodide) 200 µg/mL RNase A. Samples were incubated for 30 min at 37 °C in the dark until analysis. DNA content was analyzed using an LSRII flow cytometer (Becton Dickinson, San Jose, CA, USA).

2.5. Effect of Ruthenium Complexes 1–3 on DNA Oxidative Damage

We pre-incubated cells with complexes 1–3, succinimide, and RuCl₃ at a concentration of 50 µM for 24 h in 37 °C in 5% CO₂, then cells were washed with PBS and incubated with H₂O₂ at 0.025 or 0.05 mM for 15 min on ice. Cell viability after incubation with H₂O₂ was in the range of 95–100% (data not shown). After incubation with H₂O₂ cells were centrifuged, suspended in LMP agarose, and spread onto a microscope slide. The slides were processed as described below in the Section 2.6.

2.6. Comet Assay

The comet assay was performed under alkaline conditions according to the procedure of Tokarz et al. [24]. A freshly prepared cell suspension in 0.75% LMP agarose dissolved in PBS was layered onto microscope slides (Superior, Germany), which were pre-coated with 0.5% NMP agarose. Then, the cells were lysed for 1 h at 4 °C in a buffer containing 2.5 M NaCl, 0.1 M EDTA, 10 mM Tris, 1% Triton X-100, pH = 10. After cell lysis, the slides were placed in an electrophoresis unit. DNA was allowed to unwind for 20 min in the solution containing 300 mM NaOH and 1 mM EDTA, pH > 13.

Electrophoretic separation was performed in the solution containing 30 mM NaOH and 1 mM EDTA, pH > 13 at an ambient temperature of 4 °C (the temperature of the running buffer did not exceed 12 °C) for 20 min at an electric field strength of 0.73 V/cm (28 mA). Then, the slides were washed in water, drained, stained with 2 µg/mL DAPI, and covered with coverslips. To prevent additional DNA damage, the procedure described above was conducted under limited light or in the dark.

2.7. Comet Analysis

The comets were observed at 200× magnification in an Eclipse fluorescence microscope (Nikon, Tokyo, Japan) attached to a COHU 4910 video camera (Cohu, Inc., San Diego, CA, USA) equipped with a UV-1 A filter block and connected to a personal computer-based image analysis system Lucia-Comet v. 6.0 (Laboratory Imaging, Praha, Czech Republic). Fifty images (comets) were randomly selected from each sample and the mean value of DNA in the comet tail was taken as an index of DNA damage (expressed in percent).

2.8. Measurement of Reactive Oxygen Species

To measure reactive oxygen species (ROS), a 2',7'-dichlorofluorescein diacetate (H₂DCFDA) probe was used. H₂DCFDA is a cell membrane-permeable non-fluorescent probe. 2',7'-dichlorofluorescein diacetate is de-esterified intracellularly and turns into highly fluorescent 2',7'-dichlorofluorescein upon oxidation. PBMCs and HL-60 cells were seeded at a density of 2.5 × 10⁶ cells/mL and 0.5 × 10⁶ cells/mL, respectively, and were incubated with ruthenium complexes 1–3, succinimide, and RuCl₃ at a concentration of 50 µM for 24 h at 37 °C in 5% CO₂. Next, the cells were washed twice with HBSS containing Ca²⁺ and Mg²⁺ and stained with 20 µM H₂DCFDA (Sigma-Aldrich, St. Louis, MO, USA) for 30 min at 37 °C in darkness. Then, the cells were washed twice with HBSS and incubated with 1 mM and 5 mM H₂O₂ at 37 °C in darkness. The intensity of fluorescence was measured after 30 min with λ_{ex} = 495 nm and λ_{em} = 530 nm using a microplate reader Synergy HT (Bio-Tek Instruments, Winooski, VT, USA). The data were analyzed according to the

following formula: $(T_x - T_0/T_0) \times 100$, where T_x is the DCF fluorescence measured at the indicated time and T_0 is the DCF fluorescence measured at the beginning of the analysis.

2.9. Measurement of SOD Activity

PBMCs and HL-60 cells were seeded at density 3×10^6 cells/mL and 1×10^6 cells/mL, respectively, in a 75 cm² cell culture flask. The cells were incubated with ruthenium complexes 1–3, succinimide, and RuCl₃ at a concentration of 50 μM for 24 h at 37 °C in 5% CO₂. Next, HL-60 cells were washed with PBS and incubated with 0.1 mM H₂O₂ for 15 min on ice. In the case of PBMCs, we used 0.25 mM H₂O₂ for 15 min at 37 °C. Next, cells were sonicated under the ice in 0.5 mL of PBS for 30 s using the 4710 Series Ultrasonic Homogenizer (Cole-Parmer Instrument Co., Chicago, IL, USA) to obtain cell lysates. SOD activity was measured using the SOD Assay Kit-WST (Dojindo, Kumamoto, Japan) by following the manufacturer's instructions. Cells lysates served as the sample solution. The mixture was placed into each well with 200 μL of WST working solution. Twenty microliters of enzyme working solution were added into each well and mixed thoroughly. The plate was incubated at 37 °C for 20 min. The absorbance was read at 450 nm using a microplate reader Synergy HT (Bio-Tek Instruments, Winooski, VT, USA).

2.10. Statistical Analysis

Data of cell viability, ROS measurement, cell cycle, and SOD activity are presented as the mean values ± standard deviation (SD) of at least three replicates. Values in the comet test are expressed as mean values + standard error of the mean (SEM) of three experiments; data from three experiments were collected and statistical parameters were calculated. Statistical analysis was performed using the Mann–Whitney test (samples with distributions departing from normality) and the Student *t*-test (normal distribution of the sample). Differences were considered statistically significant when the *p*-value was <0.05.

3. Results

3.1. Cell Viability

All experiments were performed with ruthenium complexes 1–3 at a concentration of 50 μM. We chose this concentration based on our previous studies in which we showed an increase in cell viability for both PBMCs and HL-60 after 24 h incubation with ruthenium complexes at 50 μM [5].

After pre-incubation, the cells were incubated with H₂O₂ for 4 h and the viability was determined with a resazurin reduction assay. We observed a significant increase ($p < 0.001$) in the viability of normal and cancer cells pre-incubated with all ruthenium complexes compared to the cells that were not pre-incubated (Figure 2). The cells that were pre-incubated with RuCl₃ under the same conditions showed a further decrease ($p < 0.001$) in viability following incubation with H₂O₂, except for the PBMCs which were incubated with H₂O₂ at 0.4 and 0.6 mM. We also observed a decrease ($p < 0.001$) in the viability of the HL-60 cells that were pre-incubated with succinimide. In the case of the normal cells, we detected the opposite effect of pre-incubation with the ligand—an increase in the viability of PBMCs compared to the cells that were only incubated with H₂O₂ at 0.4 and 0.6 mM ($p < 0.001$).

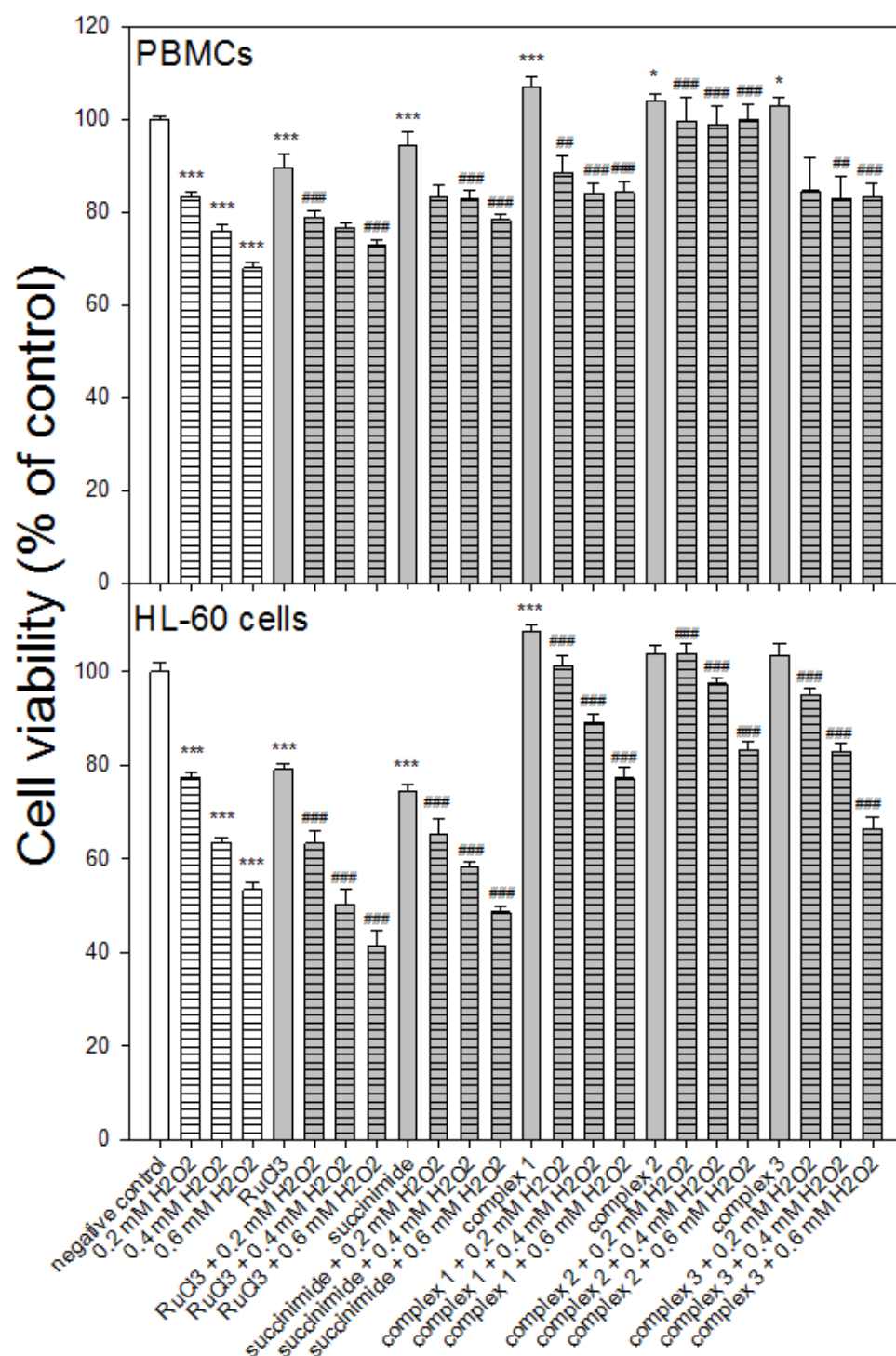


Figure 2. Effect of ruthenium complexes 1–3 at 50 μ M on the viability of PBMCs and HL-60 cells incubated with H₂O₂. The viability for individual samples was calculated relative to negative control (untreated cells) \pm SD. Cell viability in the control was taken as 100%, $n = 6$, * $p < 0.05$, *** $p < 0.001$ vs. negative control, ## $p < 0.01$, ### $p < 0.001$ vs. H₂O₂.

3.2. Cell Cycle

After incubation of HL-60 cells with 0.1 mM H₂O₂, we observed an increase in the number of cells in the sub-G1 ($p < 0.001$), S ($p < 0.001$) and G2/M ($p < 0.01$) phases of the cell cycle and a decrease in the G0/G1 phase ($p < 0.001$) compared to the control cells (Table 1). H₂O₂ at a higher concentration causes a further growth of HL-60 cells in the sub-G1 phase

($p < 0.001$) and a significant decrease in the number of cells in the phases G0/G1 ($p < 0.01$) and G2/M ($p < 0.01$).

We showed a decrease in the number of cells in the sub-G1 phase after pre-incubation with ruthenium complexes 1–3 compared to the cells incubated only with H₂O₂, both at 0.1 and 0.2 mM ($p < 0.001$). A similar decrease in the number of cells was observed in the S phase ($p < 0.001$). In addition, we demonstrated cell arrest in the G2/M phase by pre-incubation of HL-60 cells with complexes 1–3 and incubation with 0.2 mM H₂O₂.

HL-60 cells that were pre-incubated with RuCl₃ or succinimide and then incubated with H₂O₂ showed similar changes in the course of the cell cycle as the cells pre-incubated with ruthenium complexes 1–3 (Table 1).

Table 1. Cell cycle distribution measured by flow cytometry using a staining with propidium iodide in HL-60 cells pre-incubated for 24 h at 37 °C with ruthenium complexes 1–3 at 50 µM and then incubated with H₂O₂ at 0.1 and 0.2 mM for 24 h at 37 °C. The cells incubated with 100 ng/mL nocodazole (NOC) for 24 h at 37 °C were the positive control.

Treatment	DNA Content %			
	Sub-G1	G0/G1	S	G2/M
negative control	1.19 ± 0.14	35.38 ± 1.64	25.66 ± 0.11	37.21 ± 1.72
positive control (NOC 100 ng/mL)	9.93 ± 2.46 ***↑	22.36 ± 6.91 *↓	21.09 ± 3.53	47.8 ± 4.22 *↑
0.1 mM H ₂ O ₂	10.39 ± 0.37 ***↑	11.27 ± 0.88 ***↓	32.73 ± 1.27 ***↑	44.79 ± 0.42 ***↑
0.2 mM H ₂ O ₂	19.83 ± 0.76 ***↑	27.43 ± 0.62 **↓	23.82 ± 2.54	28.84 ± 2.38 **↓
RuCl ₃	2.02 ± 0.43	35.28 ± 2.03	29.87 ± 0.17	32.5 ± 2.42
RuCl ₃ + 0.1 mM H ₂ O ₂	4.73 ± 0.55 ###↓	39.25 ± 0.4 ###↑	26.12 ± 0.35 ###↓	30.02 ± 0.79 ###↓
RuCl ₃ + 0.2 mM H ₂ O ₂	14.01 ± 0.98 ##↓	29.15 ± 1.48	11.6 ± 0.31 ###↓	45.37 ± 1.28 ###↑
succinimide	2.31 ± 0.33	44.42 ± 3.01 *↑	28.48 ± 2.02	24.17 ± 1.63 ***↓
succinimide + 0.1 mM H ₂ O ₂	2.07 ± 0.86 ###↓	41.95 ± 3.29 ###↑	22.63 ± 3.7 ###↓	33.17 ± 1.92 ###↓
succinimide + 0.2 mM H ₂ O ₂	5.12 ± 0.84 ###↓	27.34 ± 2.58	10.76 ± 0.15 ###↓	56.63 ± 1.66 ###↑
complex 1	1.76 ± 0.13	48.81 ± 3.48 **↑	27.59 ± 3.97	21.48 ± 1.00 ***↓
complex 1 + 0.1 mM H ₂ O ₂	2.22 ± 0.36 ###↓	41.71 ± 1.21 ###↑	20.29 ± 2.95 ###↓	35.32 ± 1.31 ###↓
complex 1 + 0.2 mM H ₂ O ₂	5.34 ± 1.42 ###↓	29.82 ± 3.78	9.72 ± 0.29 ###↓	54.96 ± 2.42 ###↑
complex 2	1.69 ± 0.13	49.3 ± 3.58 **↑	26.85 ± 3.54	21.24 ± 0.29 ***↓
complex 2 + 0.1 mM H ₂ O ₂	2.5 ± 0.56 ###↓	40.92 ± 1.8 ###↑	20.59 ± 2.28 ###↓	35.59 ± 0.53 ###↓
complex 2 + 0.2 mM H ₂ O ₂	6.64 ± 1.05 ###↓	27.92 ± 0.87	11.3 ± 0.62 ###↓	54.24 ± 0.92 ###↑
complex 3	1.76 ± 0.17	51.4 ± 0.78 ***↑	25.21 ± 0.66	21.65 ± 0.38 ***↓
complex 3 + 0.1 mM H ₂ O ₂	2.25 ± 0.15 ###↓	43.67 ± 1.54 ###↑	18.11 ± 1.76 ###↓	35.86 ± 1.68 ###↓
complex 3 + 0.2 mM H ₂ O ₂	4.95 ± 1.23 ###↓	29.35 ± 4.14	9.5 ± 1.06 ###↓	56.07 ± 2.53 ###↑

The table shows mean results ± SD, $n = 3$; * $p < 0.05$, ** $p < 0.01$, *** $p < 0.001$ vs. negative control. ## $p < 0.01$, ### $p < 0.001$ vs. 0.1 or 0.2 mM H₂O₂.

3.3. DNA Oxidative Damage

We induced DNA oxidative damage in PBMCs and HL-60 cells using H₂O₂ at two concentrations of 0.025 and 0.05 mM. Then we investigated the influence of pre-incubation with ruthenium complexes 1–3 on oxidative DNA damage (Figure 3). In the PBMCs we observed a statistically significant decrease in oxidative DNA damage for complex 1 ($p < 0.001$) and complex 2 ($p < 0.05$), but only in the case of incubation with H₂O₂ at 0.05 mM (Figure 3). After incubation of the PBMCs with H₂O₂ at a lower concentration of 0.025 mM, we did not observe any of the complexes influencing the level of DNA oxidative damage.

In the case of the pre-incubation of the PBMCs with both RuCl_3 and succinimide, we did not detect changes in the level of DNA oxidative damage induced by H_2O_2 ($p > 0.05$).

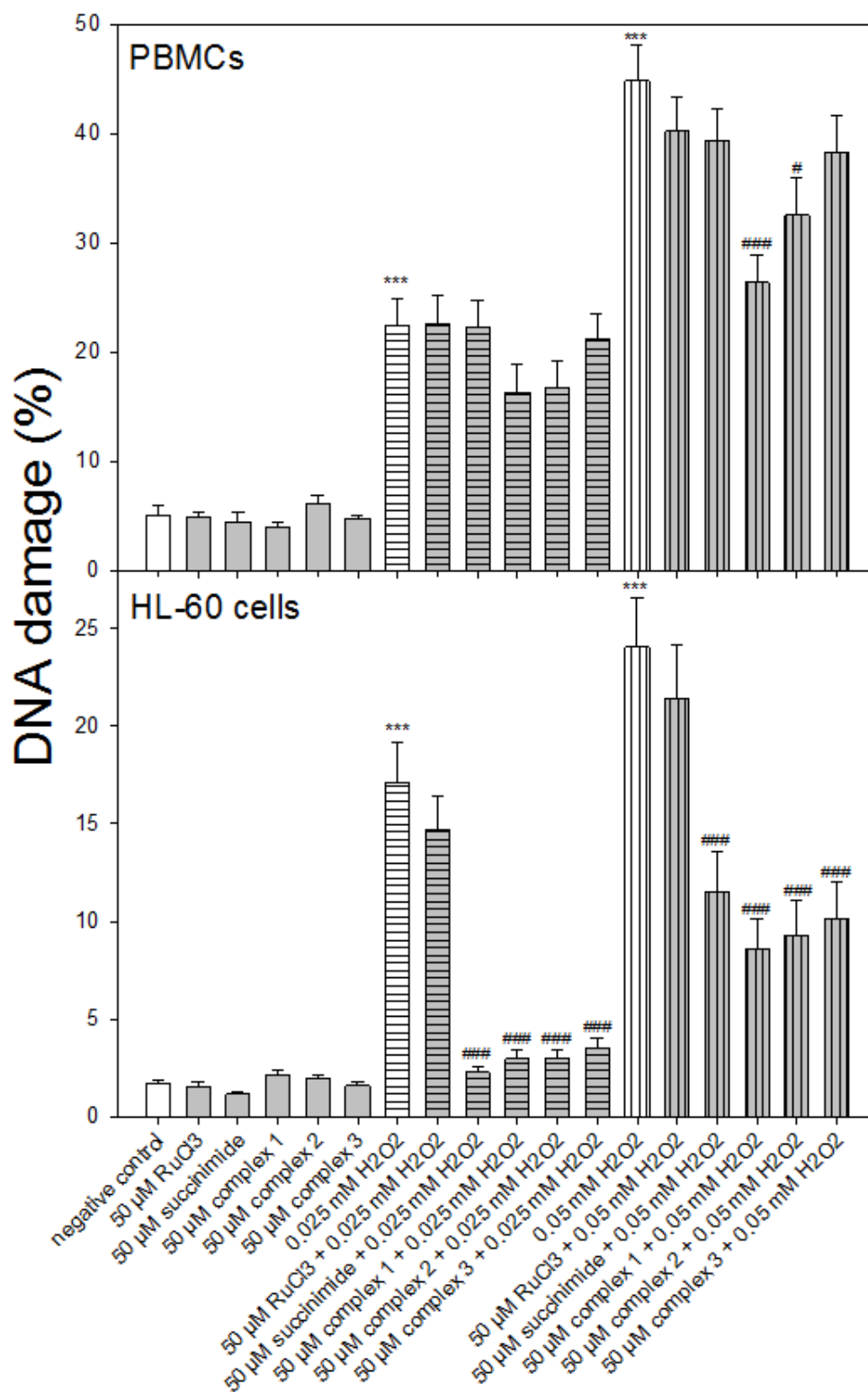


Figure 3. Effect of ruthenium complexes 1–3 at 50 μM on H_2O_2 -induced DNA damage in PBMCs and HL-60. The figures show mean results \pm SEM, $n = 100$; *** $p < 0.001$ vs. negative control; # $p < 0.05$, ### $p < 0.001$ vs. H_2O_2 .

In the experiment with HL-60 cells, we detected a significant decrease in oxidative DNA damage induced by H_2O_2 at 0.025 and 0.05 mM for all ruthenium complexes ($p < 0.001$) (Figure 3). We showed a similar effect—reduction of DNA damage in the cells pre-incubated with succinimide and then incubated with H_2O_2 at both 0.025 and 0.05 mM concentrations. In the HL-60 cells that were pre-incubated with RuCl_3 , we did not indicate any change in the oxidative DNA damage level ($p > 0.05$).

3.4. Reactive Oxygen Species Level

We used an $\text{H}_2\text{DCF-DA}$ probe to determine the effect of ruthenium complexes 1–3 on reactive oxygen species (ROS) induced by H_2O_2 at concentrations of 1 and 5 mM (Figure 4). In the case of PBMCs, we observed a decrease ($p < 0.001$) in the level of ROS for complexes 1 and 2 and 1 mM H_2O_2 (Figure 4). In contrast, complex 3 increased the level of H_2O_2 induced ROS ($p < 0.001$). A similar effect to the one found in complex 3 was observed in the PBMCs pre-incubated with succinimide and then incubated with 5 mM H_2O_2 ($p < 0.001$). Complex 2 has the greatest potential to scavenge ROS in normal cells; it also reduced endogenous ROS levels ($p < 0.001$).

In HL-60 cells, we clearly showed a significant reduction ($p < 0.001$) in ROS levels by all ruthenium complexes (Figure 4). We also observed a similar effect in the HL-60 cells pre-incubated with succinimide and then incubated with H_2O_2 at 1 mM ($p < 0.001$) and 5 mM ($p < 0.01$). All ruthenium complexes and succinimide significantly reduced endogenous ROS levels in contrast to RuCl_3 .

3.5. SOD Activity

In this experiment, we investigated the influence of ruthenium complexes on SOD activity under oxidative stress conditions (Figure 5). First, of all, we observed a decrease in SOD activity ($p < 0.001$) after the incubation of PBMCs (Figure 4) and HL-60 cells (Figure 5) with H_2O_2 , which corresponds with the results of other research [25,26]. It should be emphasized that in the case of the incubation of HL-60 cells with 0.1 mM H_2O_2 , we observed a decrease in SOD activity to 50%, whereas in the case of PBMCs the SOD activity decreased only to a level of about 93% after the use of 0.25 mM H_2O_2 . Further increasing the concentration of H_2O_2 to 0.6 mM did not cause any further inhibition of SOD activity in these cells (data not shown).

Our studies clearly showed that all ruthenium complexes increased SOD activity ($p < 0.001$) in HL-60 cells treated with H_2O_2 (Figure 5). We observed a similar effect after the pre-incubation of these cells with succinimide ($p < 0.001$). In the case of HL-60 cells pre-incubated with 50 μM RuCl_3 , we did not detect any changes in SOD activity compared to the cells that were not pre-incubated with RuCl_3 . In the case of PBMCs, we observed an increase in SOD activity ($p < 0.001$) after pre-incubation with complexes 1 and 2. Complex 3 as well as RuCl_3 and succinimide did not increase SOD activity ($p > 0.05$) (Figure 5).

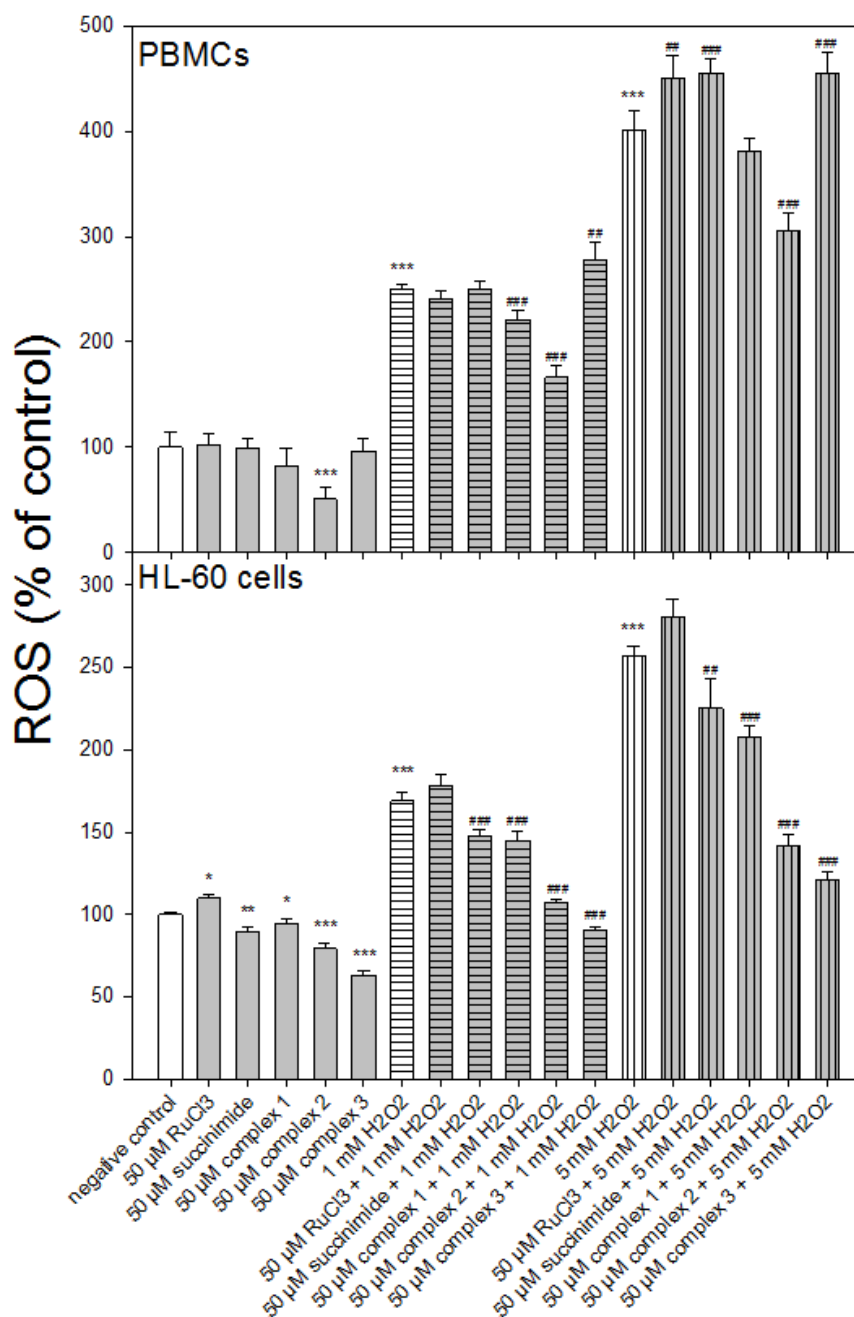


Figure 4. Changes in reactive oxygen species (ROS) level in PBMCs and HL-60 cells pre-incubated with ruthenium complexes 1–3 at 50 μ M for 24 h at 37 $^{\circ}$ C and then incubated with 1 mM or 5 mM H₂O₂ at 37 $^{\circ}$ C. Each value represents the mean \pm SD, $n = 6$; * $p < 0.05$, ** $p < 0.01$, *** $p < 0.001$ vs. negative control; ## $p < 0.01$, ### $p < 0.001$ vs. H₂O₂.

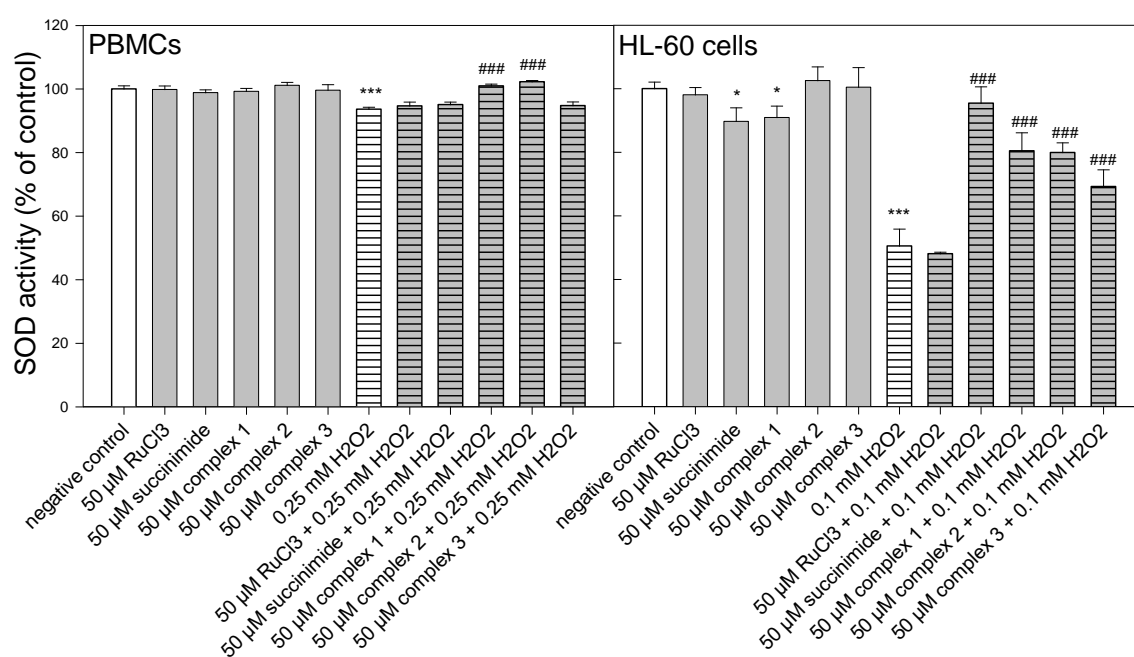


Figure 5. Superoxide dismutase activity in PBMCs and HL-60 cells pre-incubated for 24 h at 37 °C with ruthenium complexes 1–3 at 50 μ M and then incubated with H₂O₂ at 0.25 mM in the case of PBMCs and 0.1 mM in the case of HL-60 cells. The figure shows the mean results \pm SD, $n = 3$; * $p < 0.05$, and *** $p < 0.001$ vs. negative control; ### $p < 0.001$ vs. H₂O₂. Data were normalized to the negative control, which was assigned as 100% of the SOD activity.

4. Discussion

Here, we investigated the antioxidant activity of three ruthenium complexes with succinimidato and phthalimidato ligands against normal PBMCs and HL-60 leukemic cells. For this purpose, we used 24 h pre-incubation of cells with the complexes and then induced oxidative stress by incubating cells with H₂O₂. A correlation and gene ontology pathway analysis identified a rigid association with genes intertwined in cell cycle progression and proliferation after cell incubation with H₂O₂ [23]. The ten most substantially correlating genes were validated using qPCR, showing complete congruency with the microarray analysis findings. Western blotting confirmed the correlation of cell cycle-related proteins negatively correlating with H₂O₂ IC₂₅. It was also shown that the top genes related to ROS production or antioxidant defense were only in modest correlation [27]. The intracellular concentration of H₂O₂ is regulated tightly, enabling its use as a cellular signaling molecule while minimizing its potential to cause cellular damage [28]. A high concentration of H₂O₂ induces necrosis and a low concentration induces apoptosis. In HL-60 cells H₂O₂-induced apoptosis is regulated by decreased BCL-2 [29]. Moreover, it was shown that H₂O₂ evoked apoptotic events through the increase of Ca²⁺ in HL-60 cells, inducing caspase -9 and -3 activation, induction of the mitochondrial permeability transition pore (mPTP), and activation of proapoptotic proteins [30].

We observed that H₂O₂ at a concentration range between 0.2 and 0.6 mM reduced the viability of normal and cancer cells (Figure 2). In addition, we observed the cell cycle arrest of HL-60 cells in the phase sub-G1 after incubation with H₂O₂ at a concentration of 0.1 and 0.2 mM (Table 1). Our results are in line with the results previously reported on the effects of H₂O₂ on the HL-60 cell cycle [30]. The arrest of cells in the sub-G1 phase may indicate apoptosis under the influence of H₂O₂. This is confirmed by our results on cell viability after incubation with H₂O₂. For both PBMCs and HL-60 cells, we observed a significant reduction in their viability. The pre-incubation of both normal and cancer cells with ruthenium complexes 1–3 increases their viability (Figure 2) and releases cells from the sub-G1 phase (Table 1).

Hydrogen peroxide, by producing hydroxyl radicals (OH^\bullet) through the interaction with metal ions near DNA, induces DNA damage such as modified bases, apurinic/aprimidinic (AP) sites, and single-strand breaks (SSBs). The addition of OH^\bullet at position C8 within the guanine ring generates the oxidative product, 8-oxo-7,8-dihydro-2'-deoxyguanosine (8-oxodG). Similarly, the addition of OH^\bullet at position C8 of deoxyadenosine generates the oxidative product 8-oxo-7,8-dihydro-2'-deoxyadenosine (8-oxodA). These radicals are capable of further reduction or oxidation forming 2,6-diamino-4-hydroxy-5-formamidopyrimidine (FapyGua) or 8-oxo-7,8-dihydroguanine (8-oxoG), in deoxyguanosine or 4,6-diamino-5-formamidopyrimidine (FapyA) or 7,8-dihydro-8-oxoadenine (8-oxoA) in deoxyadenosine. Another prevalent oxidative product is thymine glycol, produced by the insertion of OH^\bullet at position C5 of the thymine rings. Similarly, another oxidation product of cytosine is cytosine glycol, which upon deamination leads to the formation of uracil glycol [31].

Here, we observed a statistically significant decrease in oxidative DNA damage in PBMCs for ruthenium complex **1** ($p < 0.001$) and ruthenium complex **2** ($p < 0.05$) (Figure 3). In the case of HL-60 cells, we noticed a significant decrease in oxidative DNA damage for all ruthenium complexes ($p < 0.001$) (Figure 3). Previously, we detected a protective effect on H_2O_2 -induced oxidative DNA damage by tricarbonyldichlororuthenium (II) dimer (CORM-2) and the CO-depleted molecule (iCORM-2) [32]. This may indicate that not only the released CO but also the iCORM-2, to which new ligands attach, have antioxidant properties. Here, we also observed that ruthenium complexes reduced the level of ROS induced by H_2O_2 in both types of cells (Figure 4). We used the fluorogenic 2',7'-dichlorodihydrofluorescein-diacetate (H_2DCFDA) probe to detect ROS. The acetate groups on H_2DCF allow for diffusion across the plasma membrane, after which both groups are cleaved by intracellular esterases to form H_2DCF . H_2DCF is reactive toward many types of oxidants, including nitrogen dioxide ($\bullet\text{NO}_2$), the carbonate radical anion ($\text{CO}_3^{\bullet-}$), the hydroxyl radical (OH^\bullet), Fe^{2+} , Cu^+ , thiyl radicals (e.g., the glutathione radical; GS^\bullet), and peroxidases (e.g., cytochrome c peroxidase) [33,34]. Importantly, none of the studied ruthenium complexes induced oxidative stress (Figure 4).

Superoxide dismutases (SODs) including MnSOD, Cu/Zn-SOD, and extracellular SOD along with catalase are composed as the first line of defense against ROS. Some studies also showed that oxidative stress downregulated MnSOD in several oxidative stress models induced by H_2O_2 and other oxidants. The oxidative stress-induced downregulation of MnSOD activity causes superoxide radical accumulation and superoxide can be converted to OH^\bullet in the presence of transition metals (e.g., Fenton reaction) [26]. Research carried out by Gottfredsen et al. [31] showed that *hsEC*-SOD is inhibited and fragmented by H_2O_2 . The enzyme was inhibited by H_2O_2 (37 °C, 1 h) in a dose-dependent manner, with an IC_{50} value of 0.8 mM and complete inhibition at ~2 mM. The mechanism of inhibition was similar to that of bovine Cu,Zn-SOD, including the oxidation of proline (Pro 112) and histidine (His 98, His 163) residues proximal to the active site Cu [35,36].

We detected that all ruthenium complexes increased SOD activity ($p < 0.001$) in HL-60 cells treated with H_2O_2 (Figure 5). We observed a similar effect after the pre-incubation of these cells with succinimide ($p < 0.001$). In the case of PBMCs, we observed an increase in SOD activity ($p < 0.001$), decreased by H_2O_2 , after pre-incubation with complexes **1** and **2** (Figure 5). We showed that ruthenium complexes **1** and **2** reversed the H_2O_2 -induced downregulation of SOD to normal levels in PBMCs. We assume that ruthenium complexes are responsible for the restoration of SOD activity in the case of PBMCs and its increase in HL-60 cells due to their ROS scavenging capacity. The numerous studies mentioned in the Introduction have shown that various ruthenium complexes synthesized in recent years have the ability to scavenge ROS and RNS [6–11,16].

Our results show that ruthenium complexes **1–3** bearing succinimidato and phthalimidato ligands at a low concentration of 50 μM protect cells against oxidative stress and do not exhibit cytotoxic activity. Here, we have experimentally confirmed our previous theoretical calculation results on the electronic structure of ruthenium complexes bearing different imidato ligands. We showed that in the case of maleimide, the HOMO-LUMO

(highest occupied molecular orbital and lowest unoccupied molecular orbital) energy gap was lower by 1.36 eV when compared with succinimide [5]. Therefore, we suppose that the antioxidant properties of ruthenium complexes, which we studied here, may be due to the high HOMO-LUMO energy gap. Our current comparative studies of ruthenium complexes bearing succimidato ligands with succinimide, and RuCl₃ indicate that the succinimide ligand, rather than the ruthenium metal center, is responsible for the antioxidant activity of complexes 1–3. We plan to undertake further electrochemical investigations of succinimide and complexes 1–3 to shed some light on this problem. Taking into account the fact that oxidative stress is involved in many human diseases, including cancer, antioxidant treatment involving new molecules that exhibit antioxidant properties in biological systems could be of potential interest from a clinical point of view.

Author Contributions: Conceptualization, M.J., B.R. and K.W.; methodology, M.J., M.K. and A.K.; investigation, M.J., M.K. and A.K.; writing—original draft preparation, M.J. and K.W.; writing—review and editing, B.R. and K.W.; visualization, M.J.; supervision, B.R. and K.W. All authors have read and agreed to the published version of the manuscript.

Funding: This research received no external funding.

Institutional Review Board Statement: The study was approved by the Committee for Research on Human Subjects of the University of Lodz (17/KBBN-UŁ/III/2019).

Informed Consent Statement: Informed consent was obtained from all subjects involved in the study.

Data Availability Statement: Data on reported results are deposited with the authors.

Acknowledgments: The authors gratefully acknowledge the University of Lodz, Poland, the Faculty of Chemistry, and the Faculty of Biology and Environmental Protection for financial support.

Conflicts of Interest: All authors declare that they have no conflicts of interest.

Sample Availability: Samples of the compounds (η^5 -cyclopentadienyl)Ru(CO)₂-*N*-methoxysuccinimidato (1), (η^5 -cyclopentadienyl)Ru(CO)₂-*N*-ethoxysuccinimidato (2), and (η^5 -cyclopentadienyl)Ru(CO)₂-*N*-phthalimidato (3) are available from the authors.

References

1. Singh, A.; Barman, P. Recent Advances in Schiff Base Ruthenium Metal Complexes: Synthesis and Applications. *Top. Curr. Chem.* **2021**, *379*, 29. [[CrossRef](#)] [[PubMed](#)]
2. Kacsir, I.; Sipos, A.; Ujlaki, G.; Buglyó, P.; Somsák, L.; Bai, P.; Bokor, É. Ruthenium Half-Sandwich Type Complexes with Bidentate Monosaccharide Ligands Show Antineoplastic Activity in Ovarian Cancer Cell Models through Reactive Oxygen Species Production. *Int. J. Mol. Sci.* **2021**, *22*, 10454. [[CrossRef](#)]
3. Mahmud, K.M.; Niloy, M.S.; Shakil, M.S.; Islam, M.A. Ruthenium Complexes: An Alternative to Platinum Drugs in Colorectal Cancer Treatment. *Pharmaceutics* **2021**, *13*, 1295. [[CrossRef](#)] [[PubMed](#)]
4. Sun, Q.; Li, Y.; Shi, H.; Wang, Y.; Zhang, J.; Zhang, Q. Ruthenium Complexes as Promising Candidates against Lung Cancer. *Molecules* **2021**, *26*, 4389. [[CrossRef](#)] [[PubMed](#)]
5. Juszczak, M.; Kluska, M.; Kosińska, A.; Palusiak, M.; Rybarczyk-Pirek, A.J.; Wzgarda-Raj, K.; Rudolf, B.; Woźniak, K. Cytotoxicity of piano-stool ruthenium cyclopentadienyl complexes bearing different imidato ligands. *Appl. Organomet. Chem.* **2022**, *36*, e6595. [[CrossRef](#)]
6. Mu, C.; Prosser, K.E.; Harrypersad, S.; MacNeil, G.A.; Panchmatia, R.; Thompson, J.R.; Sinha, S.; Warren, J.J.; Walsby, C.J. Activation by Oxidation: Ferrocene-Functionalized Ru(II)-Arene Complexes with Anticancer, Antibacterial, and Antioxidant Properties. *Inorg. Chem.* **2018**, *57*, 15247–15261. [[CrossRef](#)]
7. Buldurun, K.; Turan, N.; Aras, A.; Mantarçı, A.; Turkan, F.; Bursal, E. Spectroscopic and Structural Characterization, Enzyme Inhibitions, and Antioxidant Effects of New Ru(II) and Ni(II) Complexes of Schiff Base. *Chem. Biodivers.* **2019**, *16*, e1900243. [[CrossRef](#)]
8. Mohankumar, A.; Devagi, G.; Shanmugam, G.; Nivitha, S.; Sundararaj, P.; Dallemer, F.; Kalaivani, P.; Prabhakaran, R. Organoruthenium(II) complexes attenuate stress in *Caenorhabditis elegans* through regulating antioxidant machinery. *Eur. J. Med. Chem.* **2019**, *168*, 123–133. [[CrossRef](#)]
9. Sasahara, G.L.; Gouveia Júnior, F.S.; Rodrigues, R.O.; Zampieri, D.S.; Fonseca, S.; Gonçalves, R.C.R.; Athaydes, B.R.; Kitagawa, R.R.; Santos, F.A.; Sousa, E.H.S.; et al. Nitro-imidazole-based ruthenium complexes with antioxidant and anti-inflammatory activities. *J. Inorg. Biochem.* **2020**, *206*, 111048. [[CrossRef](#)]

10. Nehru, S.; Veeralakshmi, S.; Kalaiselvam, S.; Subin David, S.P.; Sandhya, J.; Arunachalam, S. Protein binding and antioxidant studies of diimine based emissive surfactant-ruthenium(II) complexes. *J. Biomol. Struct. Dyn.* **2021**, *39*, 1535–1546. [[CrossRef](#)]
11. Maikoo, S.; Chakraborty, A.; Vukea, N.; Dingle, L.M.K.; Samson, W.J.; de la Mare, J.A.; Edkins, A.L.; Booyesen, I.N. Ruthenium complexes with mono- or bis-heterocyclic chelates: DNA/BSA binding, antioxidant and anticancer studies. *J. Biomol. Struct. Dyn.* **2021**, *39*, 4077–4088. [[CrossRef](#)] [[PubMed](#)]
12. Elsayed, S.A.; Badr, H.E.; di Biase, A.; El-Hendawy, A.M. Synthesis, characterization of ruthenium(II), nickel(II), palladium(II), and platinum(II) triphenylphosphine-based complexes bearing an ONS-donor chelating agent: Interaction with biomolecules, antioxidant, in vitro cytotoxic, apoptotic activity and cell cycle analysis. *J. Inorg. Biochem.* **2021**, *223*, 111549. [[CrossRef](#)] [[PubMed](#)]
13. Santos, N.E.; Braga, S.S. Redesigning Nature: Ruthenium Flavonoid Complexes with Antitumour, Antimicrobial and Cardioprotective Activities. *Molecules* **2021**, *26*, 4544. [[CrossRef](#)] [[PubMed](#)]
14. Cuccioloni, M.; Bonfili, L.; Mozzicafreddo, M.; Cecarini, V.; Pettinari, R.; Condello, F.; Pettinari, C.; Marchetti, F.; Angeletti, M.; Eleuteri, A.M. A ruthenium derivative of quercetin with enhanced cholesterol-lowering activity. *RSC Adv.* **2016**, *6*, 39636–39641. [[CrossRef](#)]
15. Ravishankar, D.; Salamah, M.; Attina, A.; Pothi, R.; Vallance, T.M.; Javed, M.; Williams, H.F.; Alzahrani, E.M.S.; Kabova, E.; Vaiyapuri, R.; et al. Ruthenium-conjugated chrysin analogues modulate platelet activity, thrombus formation and haemostasis with enhanced efficacy. *Sci. Rep.* **2017**, *7*, 5738. [[CrossRef](#)]
16. Mabuza, L.P.; Gamede, M.W.; Maikoo, S.; Booyesen, I.N.; Ngubane, P.S.; Khathi, A. Cardioprotective effects of a ruthenium (II) Schiff base complex in diet-induced prediabetic rats. *Diabetes Metab. Syndr. Obes.* **2019**, *12*, 217–223. [[CrossRef](#)]
17. Sadiq, A.; Mahmood, F.; Ullah, F.; Ayaz, M.; Ahmad, S.; Haq, F.U.; Khan, G.; Jan, M.S. Synthesis, anticholinesterase and antioxidant potentials of ketoesters derivatives of succinimides: A possible role in the management of Alzheimer's. *Chem. Cent. J.* **2015**, *9*, 31. [[CrossRef](#)] [[PubMed](#)]
18. Hussain, F.; Khan, Z.; Jan, M.S.; Ahmad, S.; Ahmad, A.; Rashid, U.; Ullah, F.; Ayaz, M.; Sadiq, A. Synthesis, in-vitro α -glucosidase inhibition, antioxidant, in-vivo antidiabetic and molecular docking studies of pyrrolidine-2,5-dione and thiazolidine-2,4-dione derivatives. *Bioorg. Chem.* **2019**, *91*, 103128. [[CrossRef](#)]
19. Ahmad, A.; Ullah, F.; Sadiq, A.; Ayaz, M.; Saeed Jan, M.; Shahid, M.; Wadood, A.; Mahmood, F.; Rashid, U.; Ullah, R.; et al. Comparative Cholinesterase, α -Glucosidase Inhibitory, Antioxidant, Molecular Docking, and Kinetic Studies on Potent Succinimide Derivatives. *Drug Des. Dev. Ther.* **2020**, *14*, 2165–2178. [[CrossRef](#)]
20. Waheed, B.; Mukarram Shah, S.M.; Hussain, F.; Khan, M.I.; Zeb, A.; Jan, M.S. Synthesis, Antioxidant, and Antidiabetic Activities of Ketone Derivatives of Succinimide. *Evid. Based Complement. Altern. Med.* **2022**, *2022*, 1445604. [[CrossRef](#)]
21. Kubicka, A.; Fomal, E.; Olejniczak, A.B.; Rybarczyk-Pirek, A.J.; Wojtulewski, S.; Rudolf, B. Oxa-Michael reaction of metallocarbonyl complexes bearing the maleimidato ligand. Reactivity studies with selected hydroxy compounds. *Polyhedron* **2016**, *107*, 38–47. [[CrossRef](#)]
22. Kosińska, A.; Wojtulewski, S.; Palusiak, M.; Tokarz, P.; Rudolf, B. A Useful Synthetic Route to N-Nonsubstituted Succinimides via Light-Induced Degradation of Metallocarbonyl Complexes. *Organometallics* **2021**, *40*, 663–673. [[CrossRef](#)]
23. O'Brien, J.; Wilson, I.; Orton, T.; Pognan, F. Investigation of the Alamar Blue (resazurin) fluorescent dye for the assessment of mammalian cell cytotoxicity. *Eur. J. Biochem.* **2000**, *267*, 5421–5426. [[CrossRef](#)] [[PubMed](#)]
24. Tokarz, P.; Piastowska-Ciesielska, A.W.; Kaarniranta, K.; Blasiak, J. All-Trans Retinoic Acid Modulates DNA Damage Response and the Expression of the VEGF-A and MKI67 Genes in ARPE-19 Cells Subjected to Oxidative Stress. *Int. J. Mol. Sci.* **2016**, *17*, 898. [[CrossRef](#)] [[PubMed](#)]
25. Sampson, J.B.; Beckman, J.S. Hydrogen peroxide damages the zinc-binding site of zinc-deficient Cu,Zn superoxide dismutase. *Arch Biochem. Biophys.* **2001**, *392*, 8–13. [[CrossRef](#)]
26. Emamgholipour, S.; Hossein-Nezhad, A.; Ansari, M. Can Melatonin Act as an Antioxidant in Hydrogen Peroxide-Induced Oxidative Stress Model in Human Peripheral Blood Mononuclear Cells? *Biochem. Res. Int.* **2016**, *2016*, 5857940. [[CrossRef](#)]
27. Bekeschus, S.; Liebelt, G.; Menz, J.; Singer, D.; Wende, K.; Schmidt, A. Cell cycle-related genes associate with sensitivity to hydrogen peroxide-induced toxicity. *Redox Biol.* **2022**, *50*, 102234. [[CrossRef](#)]
28. Heo, S.; Kim, S.; Kang, D. The Role of Hydrogen Peroxide and Peroxiredoxins throughout the Cell Cycle. *Antioxidants* **2020**, *9*, 280. [[CrossRef](#)]
29. Lee, J.E.; Sohn, J.; Lee, J.H.; Lee, K.C.; Son, C.S.; Tockgo, Y.C. Regulation of bcl-2 family in hydrogen peroxide-induced apoptosis in human leukemia HL-60 cells. *Exp. Mol. Med.* **2000**, *32*, 42–46. [[CrossRef](#)]
30. Bejarano, I.; Espino, J.; González-Flores, D.; Casado, J.G.; Redondo, P.C.; Rosado, J.A.; Barriga, C.; Pariente, J.A.; Rodríguez, A.B. Role of Calcium Signals on Hydrogen Peroxide-Induced Apoptosis in Human Myeloid HL-60 Cells. *Int. J. Biomed. Sci. IJBS* **2009**, *5*, 246–256.
31. Barnes, J.L.; Zubair, M.; John, K.; Poirier, M.C.; Martin, F.L. Carcinogens and DNA damage. *Biochem. Soc. Trans.* **2018**, *46*, 1213–1224. [[CrossRef](#)] [[PubMed](#)]
32. Juszcak, M.; Kluska, M.; Wysokiński, D.; Woźniak, K. DNA damage and antioxidant properties of CORM-2 in normal and cancer cells. *Sci. Rep.* **2020**, *10*, 12200. [[CrossRef](#)] [[PubMed](#)]
33. Wrona, M.; Patel, K.; Wardman, P. Reactivity of 2',7'-dichlorodihydrofluorescein and dihydrorhodamine 123 and their oxidized forms toward carbonate, nitrogen dioxide, and hydroxyl radicals. *Free Radic. Biol. Med.* **2005**, *38*, 262–270. [[CrossRef](#)]

34. Reiniers, M.J.; de Haan, L.R.; Reeskamp, L.F.; Broekgaarden, M.; van Golen, R.F.; Heger, M. Analysis and Optimization of Conditions for the Use of 2',7'-Dichlorofluorescein Diacetate in Cultured Hepatocytes. *Antioxidants* **2021**, *10*, 674. [[CrossRef](#)] [[PubMed](#)]
35. Gottfredsen, R.H.; Larsen, U.G.; Enghild, J.J.; Petersen, S.V. Hydrogen peroxide induce modifications of human extracellular superoxide dismutase that results in enzyme inhibition. *Redox Biol.* **2013**, *1*, 24–31. [[CrossRef](#)]
36. Lewandowski, L.; Kepinska, M.; Milnerowicz, H. Inhibition of copper-zinc superoxide dismutase activity by selected environmental xenobiotics. *Environ. Toxicol. Pharmacol.* **2018**, *58*, 105–113. [[CrossRef](#)]